

# P12.4 CHARACTERISTICS OF RUC VERTICAL WIND PROFILES NEAR SUPERCELLS

PAUL MARKOWSKI,\* CHRISTINA HANNON, JEFF FRAME, ELISE LANCASTER, AND ALBERT PIETRYCHA

*Department of Meteorology, Pennsylvania State University, University Park, PA*

ROGER EDWARDS AND RICHARD THOMPSON

*Storm Prediction Center, Norman, OK*

## 1. Introduction

Distinguishing tornadic supercell environments from those associated with nontornadic supercells is among the most daunting challenges currently facing severe storms forecasters. In this paper we present preliminary results of a study of characteristics of nontornadic and tornadic supercell hodographs derived from 40-km Rapid Update Cycle (RUC) analyses.

One motivation for this study is the relatively recent availability of hourly conditions from analysis systems that initialize numerical weather prediction models (e.g., the RUC, which has been used herein). Although analyses are sensitive to the accuracy of short-term forecasts made by a numerical model, there are some advantages to using model analysis data. The primary advantage is the superior temporal and spatial resolution compared to that of the upper-air observing network, which permits the comparison of model analysis profiles obtained from the same storm-relative (s-r) location in space and time from case to case. Thus, the troublesome issue of defining what constitutes a suitable “proximity” sounding is somewhat circumvented. The availability of thermodynamic and wind profile information at a large number of grid points and times also facilitates the assembly of a large number of cases in far less time than if only observed soundings within relatively close proximity to an event were acceptable.

We also are motivated by the need for a comparison of hodograph characteristics between tornadic and nontornadic supercell environments over the entire troposphere. Several investigators have examined mean wind profiles associated with tornadic supercells (e.g., Darkow 1969; Maddox 1976; Darkow and McCann 1977; Kerr and Darkow 1996), but these have not yet been systematically compared to mean wind profiles associated with nontornadic supercells. Some other studies have compared tornadic and nontornadic wind profile characteristics (e.g., Brooks et al. 1994a; Rasmusussen and Blanchard 1998; Thompson 1998), but only at a few levels, and only for a relatively limited number of parameters.

It will be shown that hodograph differences are most apparent below 1 km. Furthermore, differences between the vertical wind profiles of tornadic and nontornadic supercells above 1 km are generally not statistically signifi-

cant, and where they are, the differences are probably too small to be reliably detected by the present sounding and wind profiler network.

## 2. Data and analysis methods

Vertical wind profiles derived from RUC analyses were obtained near approximately 450 supercells nationwide from 1999–2001. Only right-moving supercells were included in the analysis. Supercells were classified as nontornadic (NT; 242 cases), “weakly tornadic” (WT; associated with F0–F1 tornadoes; 154 cases), and “strongly tornadic” (ST; associated with F2–F5 tornadoes; 55 cases). For each class of supercells, vertical profiles of mean and standard deviation values for a number of parameters related to environmental wind speed and wind shear were computed. All variable definitions are consistent with those used by Davies-Jones (1984), and their relationship to the hodograph can be viewed in Fig. 1.

Figure 2 contains profiles of ground-relative (g-r) wind speed  $|\mathbf{v}|$ , s-r wind speed  $|\mathbf{v} - \mathbf{c}|$ , vertical wind shear magnitude  $|d\mathbf{v}/dz|$ , and negative hodograph curvature  $-d\phi/dz$  (positive values indicate clockwise turning of the shear vector,  $d\mathbf{v}/dz$ ), where  $\mathbf{v}(z) = [u(z), v(z)]$  is the environmental horizontal wind vector,  $\mathbf{c}$  is the observed storm motion, and  $\phi(z)$  describes the orientation of the wind shear.

Figure 3 contains profiles of crosswise vorticity  $\omega_c$  ( $= d|\mathbf{v} - \mathbf{c}|/dz$ ), streamwise vorticity  $\omega_s$  ( $= -|\mathbf{v} - \mathbf{c}|d\psi/dz$ ), g-r helicity (GRH) density  $\mathbf{v} \cdot \boldsymbol{\omega}$ , and s-r helicity (SRH) density  $(\mathbf{v} - \mathbf{c}) \cdot \boldsymbol{\omega}$ . The GRH (SRH) density is the integrand of GRH (SRH); thus, the area to the left of the  $\mathbf{v} \cdot \boldsymbol{\omega}$  [ $(\mathbf{v} - \mathbf{c}) \cdot \boldsymbol{\omega}$ ] profiles represents GRH (SRH), and the  $\mathbf{v} \cdot \boldsymbol{\omega}$  [ $(\mathbf{v} - \mathbf{c}) \cdot \boldsymbol{\omega}$ ] profiles provide information about the vertical distribution of GRH (SRH).

Mean hodographs also were constructed for each of the three classes of supercells (Fig. 4). Prior to averaging, the hodograph from each case underwent a transformation involving the removal of the 0–6 km mean wind, followed by a rotation of the hodograph so that the bulk Richardson number shear vector (the vector difference between the mean winds in the 0–500 m and 0–6 km layers) was oriented from west to east. The 0–6 km mean wind was averaged over all of the cases in each supercell class, and this mean hodograph translation (different for each supercell class) was added to the mean hodograph of each class prior to constructing Fig. 4.

Although there are many ways to transform

\*Corresponding author address: Dr. Paul Markowski, Department of Meteorology, Pennsylvania State University, 503 Walker Building, University Park, PA 16802; e-mail: pmarkowski@psu.edu.

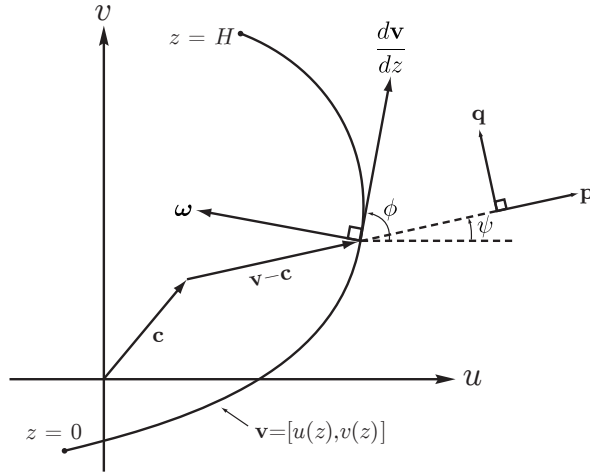


FIG. 1. Diagram of a hodograph  $[u(z), v(z)]$  depicting the storm motion vector  $\mathbf{c}$ , s-r wind vector  $\mathbf{v} - \mathbf{c}$ , vertical wind shear vector  $d\mathbf{v}/dz$ , environmental horizontal vorticity vector  $\boldsymbol{\omega}$ , and the relationships between  $\mathbf{v} - \mathbf{c}$  and  $\psi$ , and  $d\mathbf{v}/dz$  and  $\phi$ . The vectors  $\mathbf{p}(z) = (\cos \psi, \sin \psi)$  and  $\mathbf{q}(z) = (-\sin \psi, \cos \psi)$  are unit vectors parallel and normal to the left of the storm-relative wind, and  $\psi(z)$  describes the orientation of the storm-relative wind. Adapted from Davies-Jones (1984).

hodographs prior to averaging, the technique used herein differs fundamentally from transformations which often have been used in the past, such as ones in which the hodograph is rotated depending on the deviation of the storm motion from due east, followed by removal of the storm motion (e.g., Darkow and McCann 1977; Kerr and Darkow 1996). Our methodology was chosen because we believe that the hodograph transformation should depend on environmental conditions rather than storm motion (i.e., two identical wind profiles should average to the same profile, regardless of storm motion differences in the two cases).

### 3. Results

Below we summarize some of the interesting differences and similarities among the ST, WT, and NT supercell classes.

*S-r wind speeds are similar through the entire troposphere in ST, WT, and NT environments.* S-r wind speed differences were  $< 2 \text{ m s}^{-1}$  at all levels except near the tropopause, where s-r wind speeds were  $\sim 2 \text{ m s}^{-1}$  weaker in ST environments compared to NT environments. The only layer in which statistically significant differences could be established at the 95% confidence level for *any* differences between profiles was in the 1000–1500 m layer, in which s-r winds were nearly  $2 \text{ m s}^{-1}$  larger in WT environments than in ST environments. Differences in s-r wind speeds are not what could be termed “meteorologically significant” in any layer; i.e., differences are less than what could be expected to be detected observationally in a real-time setting (storm motion estimates alone are probably associated with  $> 2 \text{ m s}^{-1}$  velocity uncertainty). It is unclear how these results can be reconciled with the simulation findings of Brooks et al. (1994b) or the Thompson (1998) findings obtained from Eta model

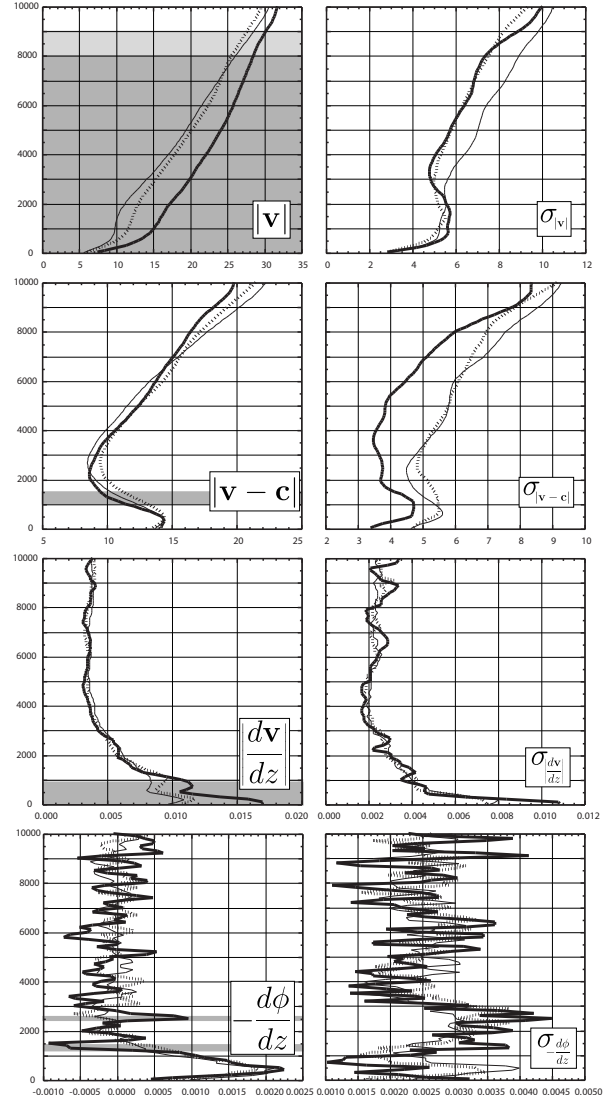


FIG. 2. (Left) Mean vertical profiles of g-r wind speed  $|\mathbf{v}|$ , s-r wind speed  $|\mathbf{v} - \mathbf{c}|$ , vertical wind shear magnitude  $|d\mathbf{v}/dz|$ , and negative hodograph curvature  $-d\phi/dz$ , from top to bottom. Height is in meters on the ordinate, and abscissa units are  $\text{m s}^{-1}$ ,  $\text{m s}^{-1}$ ,  $\text{s}^{-1}$ , and  $\text{rad m}^{-1}$ , respectively. Bold, solid profiles are associated with ST environments; bold, dotted profiles are associated with WT environments (associated with F0–F1 tornadoes); fine, solid profiles are associated with NT environments. Light gray shading denotes layers in which the mean ST value differs from the NT value at the 95% confidence level, and dark gray shading denotes layers in which the mean ST value differs from the WT value at the 95% confidence level. (Right) Standard deviation profiles for the parameters displayed on the left. Units are the same as on the left, as are the lines used to denote supercell type.

analyses.

*G-r winds are faster in ST environments than WT and NT environments.* On average, speeds in ST environments are  $5$  ( $4$ )  $\text{m s}^{-1}$  larger than speeds in NT (WT) environments. We speculate that the larger g-r winds may give rise to larger low-level vertical wind shear due to friction near the ground (simulations conducted with a free-slip lower boundary yield identical results when the

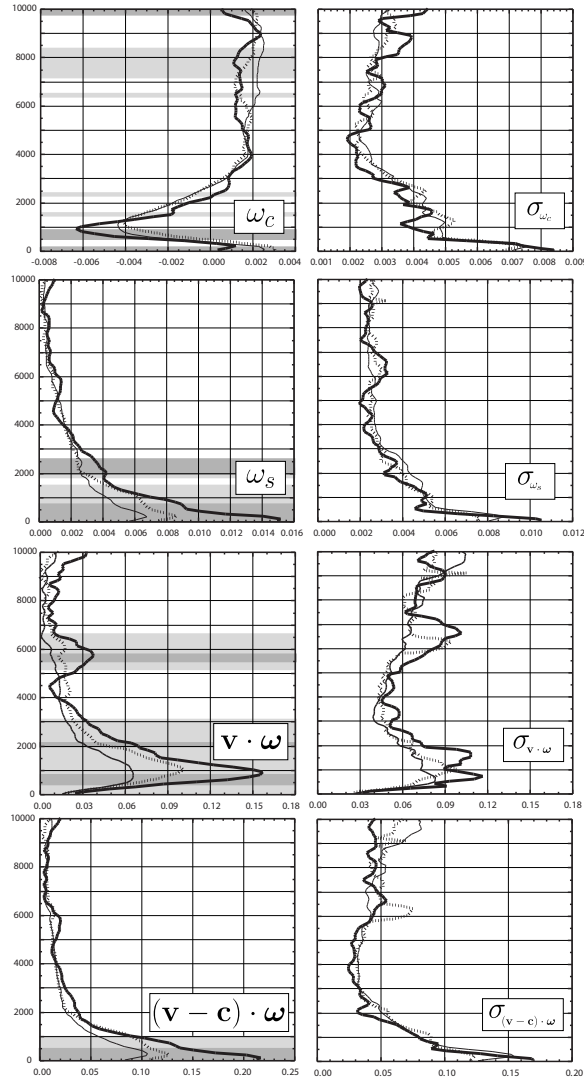


FIG. 3. (Left) Mean and standard deviation profiles (as in Fig. 2), but for crosswise vorticity  $\omega_c$ , streamwise vorticity  $\omega_s$ , GRH density  $\mathbf{v} \cdot \boldsymbol{\omega}$ , and SRH density  $(\mathbf{v} - \mathbf{c}) \cdot \boldsymbol{\omega}$ . Height is in meters on the ordinate, and abscissa units are  $\text{s}^{-1}$ ,  $\text{s}^{-1}$ ,  $\text{m s}^{-2}$ , and  $\text{m s}^{-2}$ , respectively. Gray shadings indicate the same statistical significance as in Fig. 2. (Right) Same as the plots on the right side of Fig. 2, but for s-r speed shear, negative s-r directional shear, GRH density, and SRH density.

hodograph is translated with respect to the origin). Or perhaps larger g-r wind speeds imply stronger large-scale dynamical forcing, and something about this type of atmosphere (yet undiscovered) is favorable for ST supercells. Strong tornadoes have long been associated with anomalously strong low-level and upper-level jets and large surface pressure gradients.

*Vertical wind shear magnitude, streamwise vorticity, and SRH density (and therefore its integral SRH) in ST environments are significantly larger than in WT and NT environments in the lowest 1 km.* The differences are largest at the surface. Above 1 km, these parameters generally are not significantly different. These results are consistent with Wicker’s (1996) numerical simulation findings that the development of low-level rota-

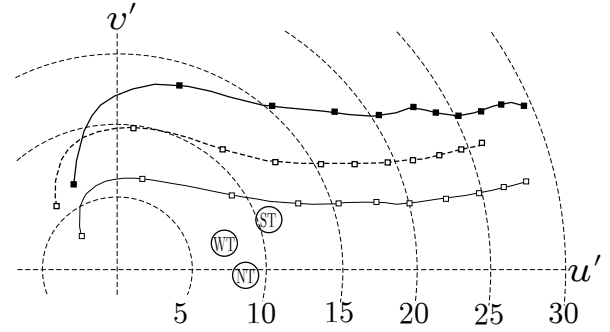


FIG. 4. Mean hodographs for strongly tornadic, weakly tornadic, and nontornadic environments (bold solid, bold dotted, and fine solid lines are used as in Figs. 2 and 3). Markings are placed along the traces at 1-km intervals. The circled “ST,” “WT,” and “NT” indicate the mean storm motions for the three supercell classes in the transformed coordinate system. Units on the speed rings are  $\text{m s}^{-1}$ .

tion in supercells is highly sensitive to the orientation of the horizontal vorticity in the lowest few hundred meters (with streamwise vorticity being much more favorable than crosswise vorticity). The results are also consistent with the Markowski et al. (1998) findings of substantially larger SRH in the lowest 1 km in tornadic versus nontornadic supercell environments. We note, however, that although the 0–1 km SRH contains the differences, the 0–3 km SRH (Davies-Jones et al. 1990) does not mask them, i.e., the SRH in the 1–3 km layer is similar in all supercell environments. [One of the reasons Davies-Jones et al. (1990) chose the 0–3 km layer for SRH calculations was the scarcity of low-level data points from wind profilers and soundings.] McCaul and Weisman (2001) also arrived at a similar conclusion regarding the importance of the vertical wind shear near the surface. Furthermore, GRH density (and therefore its integral GRH) is substantially larger in ST cases compared to WT and NT cases in roughly the 500–1500 m layer, perhaps implying stronger warm advection in ST environments (this depends on the degree of ageostrophy in ST versus WT/NT environments). These differences, along with the differences in  $|d\mathbf{v}/dz|$  in the lowest 1 km, are perhaps especially noteworthy because they are insensitive to storm motion.

*The differences between WT and NT environments typically are quite small and generally are not statistically significant.* For example,  $|d\mathbf{v}/dz|$  differences between NT and WT supercells are not statistically significant at any level. This perhaps is not terribly surprising—even on storm scales observed during recent field experiments using mobile in situ sensors and radar, many kinematic traits of WT and NT supercells have been virtually indistinguishable (e.g., Trapp 1999; Wakimoto and Cai 2000; Markowski et al. 2002). In layers in which differences in hodograph parameters are observed between WT and NT environments, the differences between the WT and NT profiles usually are smaller than the differences between ST and WT profiles.

*The shapes of the mean hodographs are virtually indistinguishable above 1 km.* The most obvious hodograph differences are the locations with respect to the origin (a manifestation of the  $|\mathbf{v}|$  differences) and the length of the

hodograph below 1 km, which leads to the  $|d\mathbf{v}/dz|$ ,  $\omega_s$ , and  $(\mathbf{v} - \mathbf{c}) \cdot \boldsymbol{\omega}$  differences noted above. The storm motions with respect to the hodographs only differ slightly, with the differences almost entirely due to the hodograph differences below 1 km [i.e., if one uses a Galilean invariant empirical storm motion predictor, such as the Rasmussen and Blanchard (1998) or Bunkers et al. (2000) techniques, the storm motions are equally well anticipated for all three mean hodographs]. Note that the s-r winds in Fig. 4 for the ST mean hodograph appear to be larger than for the NT mean hodograph. This is a fluke of the averaging, due to the fact that  $|\mathbf{v} - \mathbf{c}| \neq |\bar{\mathbf{v}} - \bar{\mathbf{c}}|$ , where  $|\mathbf{v} - \mathbf{c}|$  is the mean s-r wind speed (displayed in Fig. 2), and  $|\bar{\mathbf{v}} - \bar{\mathbf{c}}|$  is the s-r wind speed obtained from the mean hodograph and mean storm motion (which can be obtained from Fig. 4).

#### 4. Final remarks

In summary, ST environments are associated with larger

- g-r wind speeds at all levels
- vertical wind shear in the lowest 1 km
- streamwise vorticity and SRH in the lowest 1 km

compared to WT and NT environments. Vertical wind profiles associated with ST, WT, and NT environments are relatively similar in terms of

- s-r wind speeds at all levels
- hodograph curvature at all levels
- crosswise vorticity at all levels

We note that there is considerable variability in the vertical profiles of the hodograph parameters. Standard deviations of many of the parameters displayed in Figs. 2 and 3 are as large as the parameters themselves. (Note that  $-d\phi/dz$  has particularly large standard deviations reflecting the fact that it is related to a second derivative of the vertical wind profile.) Furthermore, we do not know how the results would be altered if the averaging were done on pressure levels rather than at fixed heights above ground level. It seems intuitive that the results would be qualitatively similar.

Some remaining questions to ponder include:

- To what extent, if any, is the finding of vertical wind shear and streamwise vorticity differences in the lowest 1 km between ST and NT/WT environments due to the interaction of ST storms with low-level baroclinic boundaries?
- Could there be any relationship between the observed wind profile differences and rear-flank downdraft thermodynamic properties, which have recently been found to differ between tornadic and nontornadic supercells?
- When wind profile characteristics such as those investigated herein are combined with thermodynamic profile characteristics, how much improvement can be gained in our ability to distinguish between supercell types? Which combinations of parameters are best?

- Should s-r wind speeds continue to be assessed in an operational setting to discriminate between tornadic and nontornadic supercells?<sup>1</sup>

Given the wind profile similarities above 1 km, there is little wonder why operationally discriminating between tornadic and nontornadic environments has been so difficult. It is believed that it may be worthwhile to develop new technologies capable of better sampling the vertical wind profile in the lowest 500–1000 m, and with much improved horizontal resolution compared to the current wind profiler demonstration network. We also believe it would be worthwhile for future numerical simulation studies to concentrate on the effects of hodograph differences in this layer, in a manner similar to that of Wicker (1996), with a realistic inclusion of surface drag. The majority of past parameter space studies probably did not have adequate vertical resolution near the ground (2–3 grid points in the lowest kilometer) to explore the sensitivity of storms to near-ground wind profile changes.

*Acknowledgments.* We are thankful for comments provided by Mr. Steve Weiss and Drs. Bob Davies-Jones, Erik Rasmussen, Jerry Straka, and Yvette Richardson.

#### REFERENCES

- Brooks, H. E., C. A. Doswell III, and J. Cooper, 1994a: On the environments of tornadic and nontornadic mesocyclones. *Wea. Forecasting*, **9**, 606–618.
- Brooks, H. E., C. A. Doswell III, and R. B. Wilhelmson, 1994b: The role of midtropospheric winds in the evolution and maintenance of low-level mesocyclones. *Mon. Wea. Rev.*, **122**, 126–136.
- , ———, and R. B. Wilhelmson, 1994b: The role of midtropospheric winds in the evolution and maintenance of low-level mesocyclones. *Mon. Wea. Rev.*, **122**, 126–136.
- Bunkers, M. J., B. A. Klimowski, J. W. Zeitler, R. L. Thompson, M. L. Weisman, 2000: Predicting supercell motion using a new hodograph technique. *Wea. Forecasting*, **15**, 61–79.
- Darkow, G. L., 1969: An analysis of over sixty tornado proximity soundings. Preprints, *Sixth Conf. on Severe Local Storms*, Chicago, Amer. Meteor. Soc., 218–221.
- , and D. W. McCann, 1977: Relative environmental winds for 121 tornado bearing storms. Preprints, *Tenth Conf. on Severe Local Storms*, Omaha, Amer. Meteor. Soc., 413–417.
- Davies-Jones, R. P., 1984: Streamwise vorticity: The origin of updraft rotation in supercell storms. *J. Atmos. Sci.*, **41**, 2991–3006.
- , D. Burgess, and M. Foster, 1990: Test of helicity as a tornado forecast parameter. Preprints, *Sixteenth Conf. on Severe Local Storms*, Kananaskis Park, Alberta, Amer. Meteor. Soc., 588–592.
- Kerr, B. W., and G. L. Darkow, 1996: S-r winds and helicity in the tornadic thunderstorm environment. *Wea. Forecasting*, **11**, 489–505.
- Maddox, R. A., 1976: An evaluation of tornado proximity wind and stability data. *Mon. Wea. Rev.*, **104**, 133–142.
- Markowski, P. M., J. M. Straka, and E. N. Rasmussen, 1998: A preliminary investigation of the importance of helicity ‘location’ in the hodograph. Preprints, *Nineteenth Conf. on Severe Local Storms*, Minneapolis, Amer. Meteor. Soc., 230–233.
- , ———, and ———, 2002: Direct surface thermodynamic measurements within the rear-flank downdrafts of nontornadic and tornadic supercells. *Mon. Wea. Rev.*, **130**, 1692–1721.
- McCaul, E. W., and M. L. Weisman, 2001: The sensitivity of simulated supercell structure and intensity to variations in the shapes of environmental buoyancy and shear profiles. *Mon. Wea. Rev.*, **129**, 664–687.
- Rasmussen, E. N., and D. O. Blanchard, 1998: A baseline climatology of sounding-derived supercell and tornado forecast parameters. *Wea. Forecasting*, **13**, 1148–1164.
- Thompson, R. L., 1998: Eta model storm-relative winds associated with tornadic and nontornadic supercells. *Wea. Forecasting*, **13**, 125–137.
- Trapp, R. J., 1999: Observations of non-tornadic low-level mesocyclones and attendant tornadogenesis failure during VORTEX. *Mon. Wea. Rev.*, **127**, 1693–1705.
- Wakimoto, R. M., and H. Cai, 2000: Analysis of a nontornadic storm during VORTEX 95. *Mon. Wea. Rev.*, **128**, 565–592.
- Wicker, L. J., 1996: The role of near surface wind shear on low-level mesocyclone generation and tornadoes. Preprints, *Eighteenth Conf. on Severe Local Storms*, San Francisco, Amer. Meteor. Soc., 115–119.

<sup>1</sup>Clearly we do not advocate neglecting low-level storm-relative wind *velocities*, for low-level streamwise vorticity and SRH are sensitive to storm-relative wind direction changes with height.